Dalton Transactions

ROYAL SOCIETY OF CHEMISTRY

PAPER

View Article Online
View Journal | View Issue

Check for updates

Cite this: *Dalton Trans.*, 2025, **54**, 3305

Leveraging N-*exo* substituents to tune the donor/acceptor properties of mesoionic imines (MIIs)†‡

Richard Rudolf,[a] Andrej Todorovski,[a] Hartmut Schubert[b] and Biprajit Sarkar *[a]

Received 14th August 2024,
Accepted 12th December 2024

DOI: 10.1039/d4dt02317j

rsc.li/dalton

In this work, we show two synthetic routes to substitute the N_{exo} position of mesoionic imines (MIIs). By Buchwald–Hartwig amination, 5-amino-1,2,3-triazoles can be arylated at the said position, showing the versatility of amino-triazoles as building blocks for MIIs. The reaction of MIIs with electrophiles (MeI, fluoro-arenes) highlights the nucleophilic nature of MIIs as even at room temperature aromatic C–F bonds can be activated with MIIs. By combining experimental methods such as Tolman/Huynh-electronic-parameter and crystallographic interpretations with theoretical calculations, we establish that MIIs expand the nucleophilicity scale of N-donors. Contrary to the flanking substituents on the triazole scaffold, the N_{exo} substituent heavily influences the donating ability of MIIs: electron-withdrawing substituents will dramatically decrease the donor strength of the MII ligand. We have now established ways to functionalise not only the triazole backbone but also the N_{exo} position. More importantly, we show here how the substitution pattern influences the electronic structure of MIIs. Such electronic tunability should make MIIs suitable for use in various fields of chemistry.

Open Access Article. Published on 27 December 2024. Downloaded on 5/3/2026 5:07:20 PM.
This article is licensed under a Creative Commons Attribution 3.0 Unported Licence.

Introduction

In recent years, mesoionic compounds with a 1,2,3-triazole core have gained much attention due to a variety of very intriguing properties[1–5] and straightforward synthetic accessibility by the Nobel Prize winning concept of CuAAC[6–13] (Cu-catalyzed azide–alkyne-cycloaddition). As the most prominent representatives of mesoionic triazole-based compounds, mesoionic carbenes (MICs),[1,3,4,14–16] mesoionic olefins (MIOs)[2] and mesoionic imines (MIIs)[5,17–20] have gained attention due to their strong ability to act as ligands for various transition metals, their intriguing reactivity towards main-group element substrates and their general tuneable properties (Chart 1).

While for MICs[1,3,4,14–16] and MIOs[2,21–24] many reports regarding synthesis and properties have been published recently, the field of MIIs has had a comparatively slower development, although recent publications demonstrate the utility of MIIs quite vividly.[17–20,25] The power of strong non-covalent hydrogen bonds could be harnessed by MIIs to induce regioselective cyclometalation reactions with Ir^{I} and Ir^{III} fragments.[17,26,27] Examination of the donor properties of MIIs by a combination of spectroscopic (*e.g.* CO-stretching frequen-

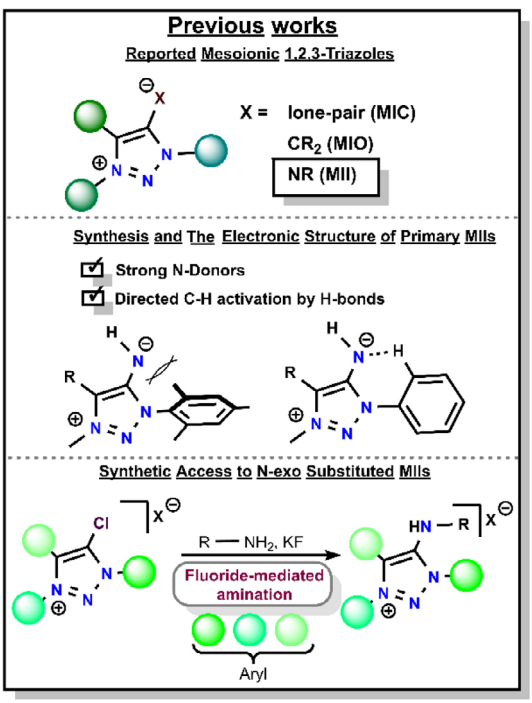

Chart 1 An overview of relevant previous work. References: [a][17,26–28] and [b].[18,19]

[a]*Institut für Anorganische Chemie, Universität Stuttgart, Pfaffenwaldring 55, 70569 Stuttgart, Germany. E-mail: biprajit.sarkar@iac.uni-stuttgart.de*
[b]*Institut für Anorganische Chemie, Universität Tübingen, Auf der Morgenstelle 18, 72076 Tübingen, Germany*

† Dedicated to Prof. P. Braunstein on the occasion of his 75th birthday.

‡ Electronic supplementary information (ESI) available. CCDC 2090873, 2104020, 2093702, 2369727, 2098233, 2363639, 2349098, 2363532, 2127404, 2393853, 2393709, 2393708, 2403053, 2405199, 2405222 and 2406185. For ESI and crystallographic data in CIF or other electronic format see DOI: https://doi.org/10.1039/d4dt02317j

Open Access Article. Published on 27 December 2024. Downloaded on 5/3/2026 5:07:20 PM.
This article is licensed under a Creative Commons Attribution 3.0 Unported Licence.

cies/TEP), theoretical and diffractometric methods revealed that MIIs act as very strong N-ligands and presumably as 2σ2π-electron donors.[17,26,27] Consequently, it is no surprise that MIIs are able to stabilise coordinatively unsaturated metals[17,26,27] or act as efficient organocatalysts.[18,19]

In previous reports from our laboratory, we concluded from diffractometric and theoretical studies that N_{exo}–H substituted (primary) MIIs can also act as potential π-accepting ligands due to their energetically accessible LUMO with π*-symmetry.[17,26–28] According to theoretical calculations, the introduction of flanking units, which can potentially engage in non-covalent H-bond interactions with the exocyclic N-fragment, lowers the LUMO energy by increasing the conjugation of the system (Chart 1). The energy of the HOMO remains unperturbed by this interaction. The π-acidity of the system can therefore be tuned by the choice of the flanking substituents.[26,27] To the best of our knowledge, there are no reports on an in-depth analysis of donor properties for N_{exo}-substituted MIIs, particularly with a focus on the N_{exo} substituents. Haraguchi and co-workers[18] studied the effect of the substituent pattern on the N_{exo} fragment regarding their activity as organocatalysts and found a direct link between basicity and catalytic activity. In their work, N_{exo} substitution of MIIs was achieved by fluoride-mediated amination reactions of 5-chloro-1,2,3-triazolium salts with differently decorated amines (Chart 1). In this regard, we now present an overview of the synthesis and characterisation of different N_{exo}-substituted MIIs and insights into the influence of the N_{exo} substitution on their electronic structure and basicity/donor capacity. For that, we decided to test if the strong nucleophilic behaviour of MIIs is a feasible starting point for derivatisation. On the other hand, we envisioned a "classical" organic transformation like the Buchwald–Hartwig amination of the amine functionality of 5-amino-triazoles[29] – valued precursors for MIIs – as a useful tool for derivatisation of N_{exo} (Scheme 1).

Results and discussion

Synthesis

The *N*-phenyl substituted triazole $\mathbf{1^{Ph}}$ was obtained by the Buchwald–Hartwig amination of bromobenzene with aminotriazole $\mathbf{1^{H}}$ (Scheme 2). Further methylation and deprotonation adopted from literature procedures[17,28] yielded the corresponding N_{exo} substituted MII $\mathbf{3^{Ph}}$. The reaction of $\mathbf{3^{H}}$ with activated fluoro-arenes yielded the corresponding *exo*-substituted MIIs $\mathbf{3^{R}}$ in yields up to 50% (Scheme 3(A)). Formally, the reaction of $\mathbf{3^{H}}$ results in the depletion of HF, which is directly quenched *in situ* by residual MII $\mathbf{3^{H}}$. The maximum calculated yield of this reaction is therefore 50% as a 1 : 1 mixture of the corresponding MII $\mathbf{3^{R}}$ and the triazolium salt $\mathbf{2^{H}}$ (present with either F^- or H_2F^- as the counter anion) is obtained.[30–33] Besides hexafluorobenzene, substrates with fewer F atoms (such as pentafluorobromobenzene or *o*-fluoronitrobenzene) could be successfully activated by $\mathbf{3^{H}}$, yielding the substituted MIIs $\mathbf{3^{R}}$. The Py-substituted derivative $\mathbf{3^{F\text{-}Py}}$ provides an additional donor atom, which makes this compound interesting for dinuclear complexes. First preliminary tests validate that $\mathbf{3^{F\text{-}Py}}$ can potentially act as a bidentate ligand (ESI Fig. S80–82‡). On the other hand, the NO_2- and Br-substituted derivatives ($\mathbf{3^{NO2\text{-}Ph}}$ and $\mathbf{3^{Br\text{-}Ph}}$) offer the opportunity for further chemical transformations.

For the synthesis of the methyl-substituted imine $\mathbf{3^{Me}}$, MII $\mathbf{3^{H}}$ was treated with methyl iodide as reported by Yan and co-workers.[20] Unlike the reactions reported for differently substituted MIIs,[20] the reaction of $\mathbf{3^{H}}$ with MeI is not selective and a mixture of different triazolium iodides ($\mathbf{2^{H}}$, $\mathbf{2^{Me}}$, and $\mathbf{2'^{Me}}$) was the result, as suggested by mass spectrometry (Scheme 2(B)). This finding is contrary to the literature report, which states a clean conversion of an MII to the corresponding Me/H-substituted triazolium salt.[20] The presence of secondary amine $\mathbf{2^{H}}$ indicates the formation of HI during the reaction, as the free imine $\mathbf{3^{H}}$ can be considered as the free base of $\mathbf{2^{H}}$. We assume that the triazolium salt $\mathbf{2^{Me}}$ depletes HI to furnish the free base $\mathbf{3^{Me}}$, which then reacts further with an equivalent of MeI resulting in the formation of $\mathbf{2'^{Me}}$ (Scheme 3B). The formation of hydrogen halides in the reaction of an NHI with an alkyl halide is a known reactivity pattern.[34] Treatment of a mixture of $\mathbf{2^{H}}$, $\mathbf{2^{Me}}$ and $\mathbf{2'^{Me}}$ with KHMDS yielded a mixture of $\mathbf{3^{H}}$ and $\mathbf{3^{Me}}$ after separation of insoluble components such as $\mathbf{2'^{Me}}$ and KI by filtration using an Et_2O solution, as suggested by ^{1}H-NMR spectroscopy (ESI Fig. S14‡). From this mixture, single crystals suitable for X-ray diffraction of $\mathbf{3^{Me}}$ were

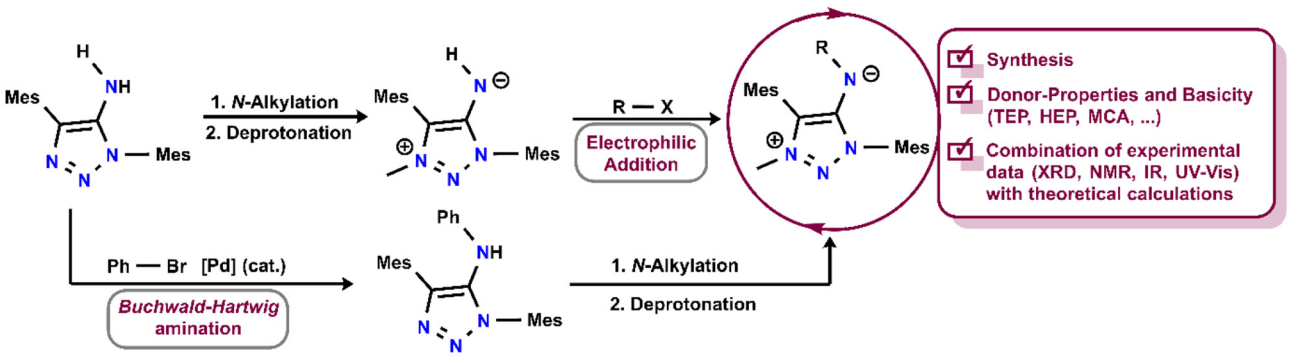

Scheme 1 Overview of the herein reported work.

This journal is © The Royal Society of Chemistry 2025

Open Access Article. Published on 27 December 2024. Downloaded on 5/3/2026 5:07:20 PM.
This article is licensed under a Creative Commons Attribution 3.0 Unported Licence.

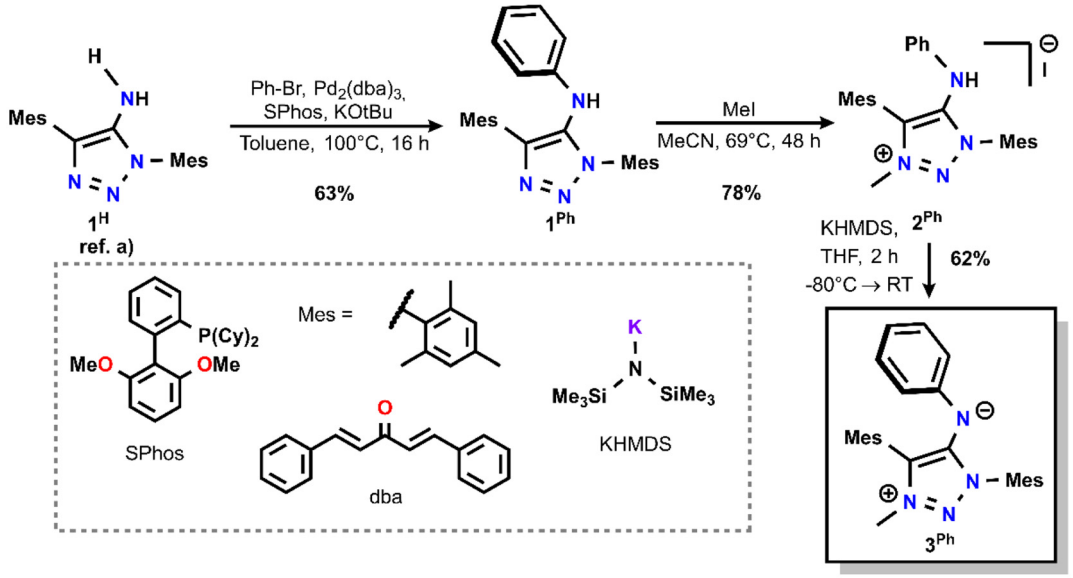

Scheme 2 Synthesis of the Ph-derivative $\mathbf{3}^{\mathbf{Ph}}$ by the Buchwald–Hartwig amination of the amino-triazole $\mathbf{1}^{\mathbf{Ph}}$ with bromobenzene followed by methylation with MeI and deprotonation of KHMDS. (Ref. a): ref. 17.

obtained at −40 °C. Further separation of $\mathbf{3}^{\mathbf{Me}}$ from $\mathbf{3}^{\mathbf{H}}$ was not possible due to their similar solubility.

Assessing the electronic structure of the MIIs 3^R using spectroscopic signatures and bond parameters

The C1–N4 ($C_{Triazole}$ and N_{exo}) bond length is a characteristic parameter for the discussion of the electronic structure of MIIs (Table 1 and Fig. 2).

With a length of 1.300(3) Å, the C1–N4 bond in the H-substituted MII $\mathbf{3}^{\mathbf{H}}$ is best characterised as a highly polarised C–N bond with double character, as discussed in earlier works by us.[17] Introduction of electron-withdrawing substituents at the *exo*-position significantly elongates this bond to up to 1.338(2) Å as seen in $\mathbf{3}^{\mathbf{F\text{-}Py}}$. This bond is now best characterised as a highly polarised C–N single bond. This trend is additionally evidenced by the shortened N4–C_R bond (C_R being the N-bound C atom of the substituent R), with the borderline case of 1.356(2) Å in $\mathbf{3}^{\mathbf{F\text{-}Py}}$. It is therefore expected that the net-donor ability and basicity will also decrease with the elongation of C1–N4/shortening of N4–C_R as the electron density is shifted from N_{exo} onto the substituent R.

Theoretically calculated methyl cation affinities (MCAs, Table 1) evidently reflect this trend, as the methyl-substituted congener $\mathbf{3}^{\mathbf{Me}}$ is supposedly the strongest base, while $\mathbf{3}^{\mathbf{F\text{-}Py}}$ is the weakest base (see the ESI for the detailed description of energies and the methods, Scheme S1 and Table S6‡). The relative basicity was further analysed by monitoring competition reactions of a MII $\mathbf{3}^{\mathbf{R}}$ (the base) with a triazolium salt $\mathbf{2}^{\mathbf{R'}}$ (the acid) with different residues (R ≠ R′) *via* ^{1}H-NMR spectroscopy (Fig. 1 top, ESI Fig. S83–88‡). According to NMR spectroscopic investigations, the reaction of $\mathbf{3}^{\mathbf{H}}$ with $\mathbf{2}^{\mathbf{Ph}}$ shows immediate proton transfer to yield $\mathbf{2}^{\mathbf{H}}$ and $\mathbf{3}^{\mathbf{Ph}}$, while no reaction was observed between $\mathbf{2}^{\mathbf{H}}$ and $\mathbf{3}^{\mathbf{Ph}}$. A more precise look into the NMR spectra (Fig. 1 (bottom) and Table 1) of the triazoles $\mathbf{1}^{\mathbf{R}}$ and triazolium salts $\mathbf{2}^{\mathbf{R}}$ fits into this discussion: the electron-withdrawing nature of the Ph substituent highly deshields the signals in the ^{1}H-NMR spectrum assigned to the N*H* protons in $\mathbf{1}^{\mathbf{Ph}}/\mathbf{2}^{\mathbf{Ph}}$ compared to $\mathbf{1}^{\mathbf{H}}/\mathbf{2}^{\mathbf{H}}$. These are indicators of a more pronounced acidity of $\mathbf{2}^{\mathbf{Ph}}$ compared to $\mathbf{2}^{\mathbf{H}}$ and conversely a lower basicity of the conjugate base $\mathbf{3}^{\mathbf{Ph}}$ compared to $\mathbf{3}^{\mathbf{H}}$. MCAs calculated for the triazoles $\mathbf{1}^{\mathbf{H}}$ and $\mathbf{1}^{\mathbf{Ph}}$ further elaborate this trend. As the reaction of $\mathbf{3}^{\mathbf{H}}$ yielded the already deprotonated products $\mathbf{3}^{\mathbf{R}}$ (R = F-Ph, F-Py, NO_2-Ph, and Br-Ph), downstream deprotonation of the triazolium salts $\mathbf{2}^{\mathbf{R}}$ (presumably with a F^- counter anion), which are formed after nucleophilic substitution of the fluoro-arene with $\mathbf{3}^{\mathbf{H}}$, with another equivalent of $\mathbf{3}^{\mathbf{H}}$ resulting in the formation of $\mathbf{2}^{\mathbf{H}}$ (presumably with a F^- counter anion) occurred (see the paragraph above on the synthesis).[30,32,33] This observation fits the trend established above that $\mathbf{3}^{\mathbf{H}}$ is a stronger base than $\mathbf{3}^{\mathbf{R}}$ (R = F-Ph, F-Py, NO_2-Ph, and Br-Ph). This is also evident from competition reactions monitored by NMR spectroscopy. Mixing either $\mathbf{3}^{\mathbf{F\text{-}Py}}$ or $\mathbf{3}^{\mathbf{F\text{-}Ph}}$ with $\mathbf{2}^{\mathbf{Ph}}$ resulted in no reaction, thus following the trend established by the bond parameters and MCAs. The electronic structure of the differently decorated MIIs was further studied by (TD)-DFT calculations (Fig. 3) in conjunction with UV-Vis spectroscopy (Fig. 4). As already discussed in previous reports,[26,27] the HOMO of MIIs is predominantly localised on the exocyclic N atom with some contribution from the triazole backbone, while the LUMO is fully localised on the triazole backbone. The herein discussed compound $\mathbf{3}^{\mathbf{R}}$ follows this trend in some respects but the substitution at the *exo*-position also alters the electronic structure strongly in some examples. The more electron-withdrawing nature of the aryl substituents introduced into the MII (R = Ph, F-Ph, F-Py, NO_2-Ph, and Br-Ph) results in the delocalisation of the HOMO into the aryl

Open Access Article. Published on 27 December 2024. Downloaded on 5/3/2026 5:07:20 PM.
This article is licensed under a Creative Commons Attribution 3.0 Unported Licence.

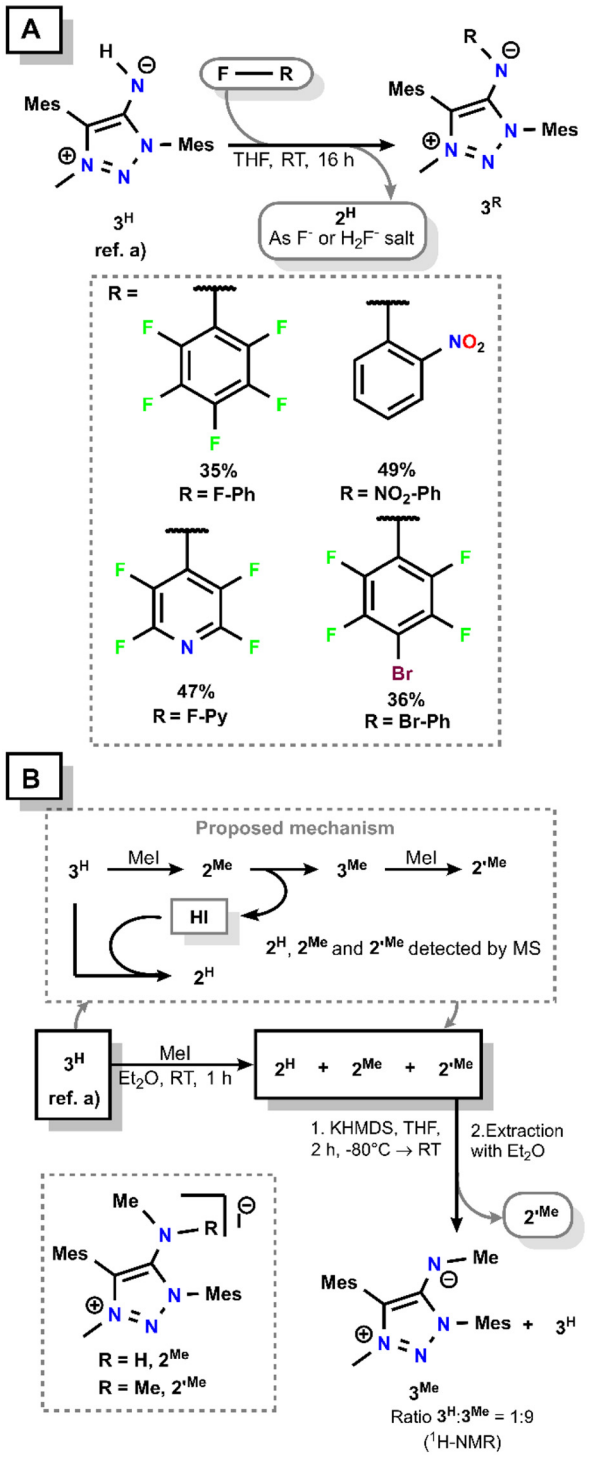

Scheme 3 A) C–F activation of different fluoro-arenes F–R with $\mathbf{3^H}$, resulting in the formation of the corresponding *N*-substituted MII $\mathbf{3^R}$ and one equivalent of triazolium salt $\mathbf{2^H}$. (B) Methylation of $\mathbf{3^H}$ with MeI and the proposed mechanism to explain the detected products of this reaction. (Ref. a): ref. 17.

substituent R, which stabilises the HOMO energy (Fig. 3 bottom). The LUMO-energy level is also decreased by the more electron-withdrawing nature of the substituent R, which is the result of the (weak) π-acidity of the substituents. In contrast to that, the LUMO of $\mathbf{3^{NO2\text{-}Ph}}$ is completely localised on the *o*-nitrobenzene moiety (Fig. 3 bottom) as this substituent acts as a substituent with a strong (−)-M effect, resulting in a strongly destabilised LUMO energy level. The HOMO is not as stabilised in the case of $\mathbf{3^{NO2\text{-}Ph}}$ as it is in the other aryl-substituted MII $\mathbf{3^R}$ (R = Ph, F-Ph, F-Py, and Br-Ph), which is rationalised as the *o*-nitrobenzene is not as σ-acidic as the other substituents. Both effects result in a relatively small HOMO–LUMO energy gap (Fig. 3).

Experimentally this can be observed by the naked eye as the compounds show very different colours as a solid and in solution (Fig. 4): $\mathbf{3^{F\text{-}Py}}$ is colourless. $\mathbf{3^{F\text{-}Ph}}$, $\mathbf{3^{Br\text{-}Ph}}$ and $\mathbf{3^H}$ have a weak orange/yellow colour. $\mathbf{3^{Ph}}$ is bright yellow and $\mathbf{3^{NO2\text{-}Ph}}$ has an intense red colour. This behaviour was further probed by UV-Vis spectroscopy. In Fig. 4, the region of the UV-Vis spectra with the absorption of the lowest energy for the compound $\mathbf{3^R}$ (R = F-Py, F-Ph, Ph, and NO_2-Ph) is shown (see ESI Fig. S76–79‡ for full spectra). From TD-DFT calculations, these absorption bands could be assigned to the corresponding HOMO–LUMO charge transfer (N_{exo}/R → triazole backbone and N_{exo} → *o*-nitrobenzene in the case of $\mathbf{3^{NO2\text{-}Ph}}$) (see the ESI‡ for further details). The maxima of these bands are red-shifted in the sequence $\mathbf{3^{F\text{-}Py}}$–$\mathbf{3^{F\text{-}Ph}}$–$\mathbf{3^{Ph}}$–$\mathbf{3^{NO2\text{-}Ph}}$, which follows the trend of the HOMO–LUMO energy gaps and the corresponding colours. With an absorption maximum at a wavelength of 361 nm,[26] $\mathbf{3^H}$ also follows this trend of the HOMO–LUMO energy gap, colour and absorption wavelength. In between the bands for $\mathbf{3^{F\text{-}Ph}}$ (λ_{max} = 358 nm) and $\mathbf{3^{Ph}}$ (λ_{max} = 392 nm), $\mathbf{3^{NO2\text{-}Ph}}$ shows another band at λ_{max} = 367 nm, which could be assigned to a HOMO → LUMO+1 transition from TD-DFT calculations. The LUMO+1 in $\mathbf{3^{NO2\text{-}Ph}}$ is mostly localised on the triazole backbone and therefore shares the same characteristics as the LUMOs in the other $\mathbf{3^R}$ compounds. The energy gap between the HOMO and LUMO+1 in $\mathbf{3^{NO2\text{-}Ph}}$ is in between the HOMO–LUMO energy gap for $\mathbf{3^{F\text{-}Ph}}$ and $\mathbf{3^{Ph}}$, thus following the already established trends.

This discussion therefore reveals the intricate effect the N_{exo} substituent has on the electronic structure of MIIs. Being in the first coordination sphere of the MII, the substitution pattern influences the electronic structure of the MIIs more heavily than the corresponding flanking substituent.[26,27] To gain further insights into this behaviour, we decided to determine the Tolman- and Huynh-electronic parameters (TEP/HEP) to provide a platform for discussion with already reported MII ligands.

Coordination to transition metals and determination of TEP/HEP

The Rh and Pd complexes ($\mathbf{3Rh^R}$/$\mathbf{3Pd^R}$) were prepared by stirring the appropriate free MII $\mathbf{3^R}$ with the appropriate dimer $[Rh(CO)_2Cl]_2$/$[(NHC)PdBr_2]_2$ overnight at room temperature in either THF ($\mathbf{3Rh^R}$) or DCM ($\mathbf{3Pd^R}$) respectively (Scheme 4).

The MII-Rh complexes $\mathbf{3Rh^R}$ (R = Ph, F-Ph, F-Py, and Br-Ph) could be isolated in satisfactory yields and characterised by spectroscopy (NMR and IR), mass spectrometry (not for

 This journal is © The Royal Society of Chemistry 2025

Open Access Article. Published on 27 December 2024. Downloaded on 5/3/2026 5:07:20 PM.
This article is licensed under a Creative Commons Attribution 3.0 Unported Licence.

Table 1 Selected bond lengths and spectroscopic data for selected compounds

Compound	δ^{1H}(–NH) [ppm]	d_{C1-N4} [Å]	$d_{N4-C(R)}$ [Å]	d_{N4-M} [Å]	d_{M-C} [Å]	TEP [cm^{-1}]	HEP [ppm]	MCA[i] [kcal mol^{-1}]	$\phi_{C1-N4-C}$ [°]
$\mathbf{1}^{H}$ [a]	3.39[c], 4.40[d]	1.362(4)	—	—	—	—	—	75.1	—
$\mathbf{1}^{Ph}$	5.06[c], 6.25[d]	1.381(1)	1.398(2)	—	—	—	—	65.8	126.8(1)
$\mathbf{2}^{H}$ [a]	5.28[c], 5.53[d]	1.363(7)	—	—	—	—	—	—	—
$\mathbf{2}^{Ph}$	8.28[c], 7.40[d]	1.363(4)	1.414(4)	—	—	—	—	—	122.1(3)
$\mathbf{3}^{H}$	3.48[a,b], 2.33[a,d]	1.300(3)[a]	—	—	—	2041[a,f]	167[e], 166[c]	108.9	—
$\mathbf{3}^{Ph}$	—	1.310(3)	1.392(3)	—	—	2044[f]	165[e]	103.0	121.0(2)
$\mathbf{3}^{Me}$	—	1.295(2)	1.441(2)	—	—	—	—	110.8	115.8(1)
$\mathbf{3}^{F-Ph}$	—	1.324(2)	1.374(2)	—	—	2048[f]	163[e]	95.7	120.2(1)
$\mathbf{3}^{F-Py}$	—	1.338(2)	1.356(2)	—	—	2049[f]	160[e]	89.9	119.9(1)
$\mathbf{3}^{NO2-Ph}$	—	1.317(2)	1.372(2)	—	—	2048[f]	161[e]	95.4	119.8(1)
$\mathbf{3}^{Br-Ph}$	—	1.328(3)	1.377(4)			2047[f]	162[e]	94.9	117.0(2)
$\mathbf{3Rh}^{Ph}$	—	1.338(4)	1.424(4)	2.104(2)[g]	1.840(3)/1.832(4)[g]	—	—	—	120.1(2)
$\mathbf{3Rh}^{F-Py}$	—	1.354(2)	1.390(2)	2.127(1)[g]	1.844(2)/1.847(2)[g]	—	—	—	120.2(1)
$\mathbf{3Rh}^{NO2-Ph}$	—	1.344(5)	1.417(5)	2.128(3)[g]	1.839(6)/1.840(7)[g]	—	—	—	117.3(3)
$\mathbf{3Rh}^{Br-Ph}$	—	1.342(8)	1.418(8)	2.114(5)[g]	1.8437(8)/1.837(9)[g]	—	—	—	117.1(5)
$\mathbf{3Pd}^{H}$	2.10[e]	1.320(6)	—	2.068(4)[h]	1.953(4)[h]	—	—	—	—
$\mathbf{3Pd}^{Ph}$	—	1.328(5)	1.427(5)	2.099(3)[h]	1.948(4)[h]	—	—	—	116.4(3)
$\mathbf{3Pd}^{F-Ph}$	—	1.340(7)	1.401(8)	2.108(4)[h]	1.944(6)[h]	—	—	—	115.7(5)
$\mathbf{3Pd}^{NO2-Ph}$	—	1.326(7)	1.402(8)	2.110(5)[h]	1.942(6)[h]	—	—	—	119.6(5)

[a] Data taken from ref. 17. [b] Recorded in C_6D_6. [c] Recorded in $CDCl_3$. [d] Recorded in CD_3CN. [e] Recorded in CD_2Cl_2. [f] Recorded in CH_2Cl_2. [g] M = Rh and C = CO (*trans*/*cis*). [h] M = Pd and C = $C_{carbene}$. [i] Level-of-theory: PBE0/def2-TZVP/CPCM(CH_2Cl_2).

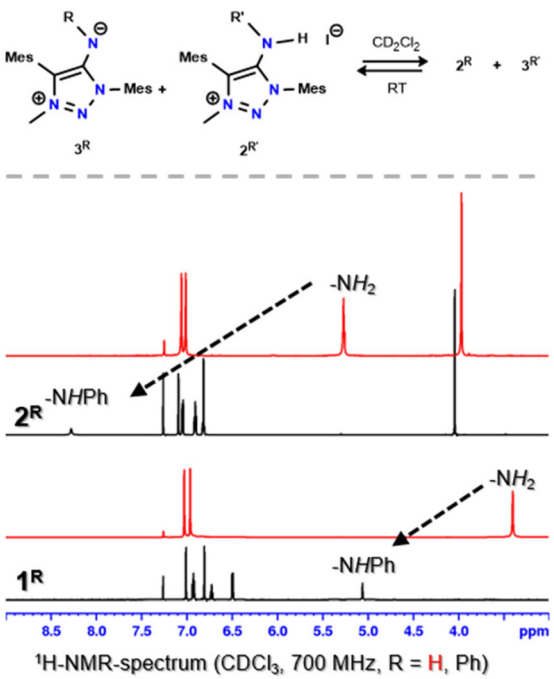

Fig. 1 Top: Performed competition reactions. Bottom: ^{1}H-NMR spectra of selected compounds. Spectra of $\mathbf{1}^{H}/\mathbf{2}^{H}$ were taken from ref. 17.

$\mathbf{3Rh}^{F-Py}$), CHN analysis and sc-XRD (not for $\mathbf{3Rh}^{F-Ph}$, Fig. 5). The isolation of the (*o*-NO_2)-Ph substituted Rh-complex $\mathbf{3Rh}^{NO2-Ph}$ proved to be troublesome. After several crystallization/precipitation steps, only sparse amounts of spectroscopically pure $\mathbf{3Rh}^{NO2-Ph}$ were obtained (see the ESI‡ for a more detailed discussion). The quantity of the obtained product was enough for ^{1}H-NMR- and IR-spectroscopic investigation but insufficient for further analyses like $^{13}C\{^1H\}$-NMR spectroscopy or CHN analysis.

In the case of the MII-Pd complexes $\mathbf{3Pd}^{R}$, only the complexes with R = H, Ph and F-Ph could be isolated in satisfactory to quantitative yields and thoroughly characterised by NMR spectroscopy, mass spectrometry (in the case of $\mathbf{3Pd}^{F-Ph}$), CHN analysis and sc-XRD (Fig. 5). For the other compounds (R = F-Py, NO_2-Ph, and Br-Ph), we observed that no full conversion of the ligands $\mathbf{3}^{R}$ and the Pd precursor was achieved during the reaction. As our attempts to separate the desired complexes $\mathbf{3Pd}^{R}$ from the corresponding ligand $\mathbf{3}^{R}$ were unsuccessful, the HEP was determined from the crude reaction mixture, which gave reasonable data in conjunction with the data obtained from the isolated complexes $\mathbf{3Pd}^{R}$ (R = H, Ph and F-Ph) and the theoretical calculations. The molecular structures in the crystals obtained for some of the complexes $\mathbf{3Pd}^{R}$ (R = Ph, H, F-Ph, and NO_2-Ph) and $\mathbf{3Rh}^{R}$ unambiguously show that the MII ligands $\mathbf{3}^{R}$ act as N-ligands *via* the exocyclic N atom as expected and reported previously by us.[17,26–28]

The stretching modes of the carbonyl ligands in the Rh complexes $\mathbf{3Rh}^{R}$ were determined by IR spectroscopy (ESI Fig. S71–75 and Table S1‡), from which the TEP[35] could be determined. The TEPs reflect the same trends stated in the previous paragraphs: the electron-withdrawing nature of the exocyclic substituent decreases the net-donor ability substantially as apparent from the TEP[17] of 2041 cm^{-1} for $\mathbf{3}^{H}$ and 2049 cm^{-1} for $\mathbf{3}^{F-Py}$. The TEP value of $\mathbf{3}^{Ph}$ with 2044 cm^{-1} is comparable to the TEPs determined for the other H-substituted MIIs $\mathbf{3}^{Fc}$ (TEP = 2044 cm^{-1}, Scheme 4 bottom)[28] and $\mathbf{3}^{Ir}$ (TEP = 2045 cm^{-1}, Scheme 4 bottom),[27] which suggest comparable net-donor abilities of the three congeners. A look into the bond parameters implies otherwise: with 2.104(2) Å, the N4–Rh bond in $\mathbf{3Rh}^{Ph}$ is much longer compared to the

Open Access Article. Published on 27 December 2024. Downloaded on 5/3/2026 5:07:20 PM.
This article is licensed under a Creative Commons Attribution 3.0 Unported Licence.

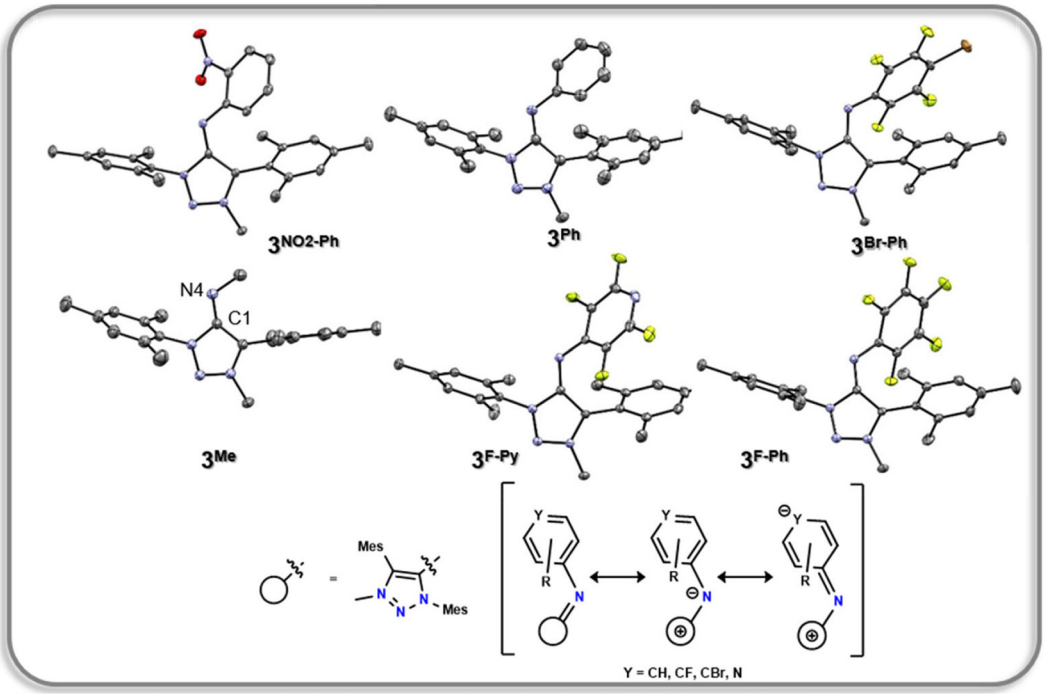

Fig. 2 Molecular structure in the crystal of the herein reported MIIs obtained by sc-XRD (single-crystal X-ray diffraction) in ORTEP-representation. Thermal ellipsoids are set to 50% probability. Protons were omitted for clarity. Bottom: Relevant canonical structures for the aryl-substituted MIIs.

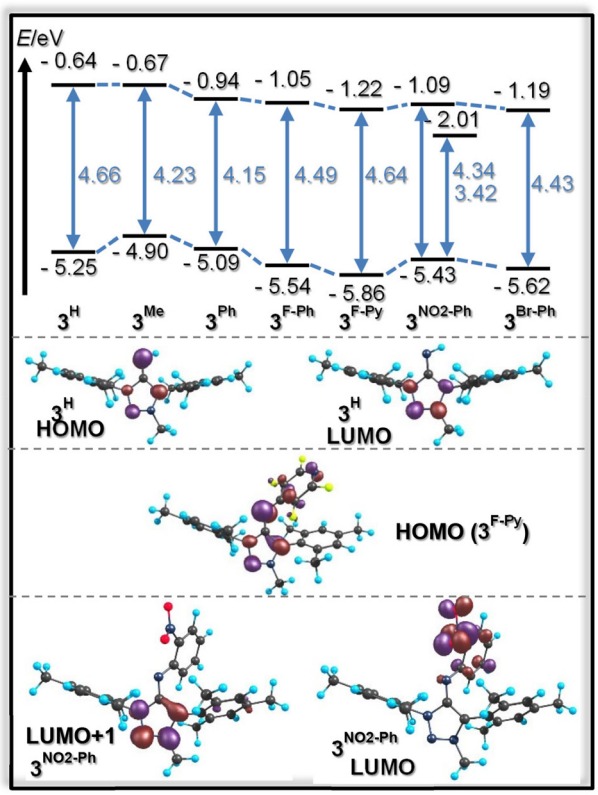

Fig. 3 MO diagram of the herein reported MIIs $\mathbf{3}^{R}$ with the energy of the frontier orbitals, the respective energy gaps and selected Kohn–Sham orbitals for selected compounds. Level-of-theory: PBE0/def2-TZVP/CPCM(CH_2Cl_2).

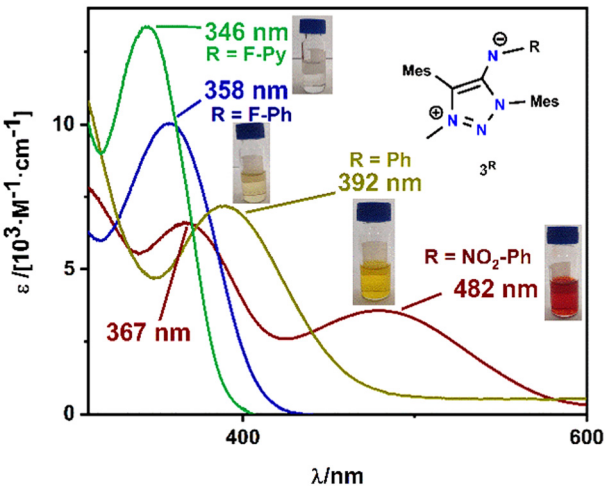

Fig. 4 Cut-outs of UV-Vis spectra of selected compounds with their respective colour. Full spectra can be found in the ESI.‡

N4–Rh bonds in the appropriate Rh complexes with either $\mathbf{3}^{Fc}$ (N4–Rh: 2.047(5) Å)[28] or $\mathbf{3}^{Ir}$ (N4–Rh: 2.075(4) Å)[27] as the MII ligand. This implies two things: (a) the TEP is not suitable for discussing donor abilities in detail, which is not a new insight but a well-known fact in the scientific community of organometallic chemistry;[35] (b) MIIs can presumably also act as acceptor ligands. In a previous report from our group, we addressed the lability of $\mathbf{3}^{Ir}$ towards moisture and poor electrophiles (acetonitrile or DCM), which contrasts with the stability

 This journal is © The Royal Society of Chemistry 2025

Open Access Article. Published on 27 December 2024. Downloaded on 5/3/2026 5:07:20 PM.
This article is licensed under a Creative Commons Attribution 3.0 Unported Licence.

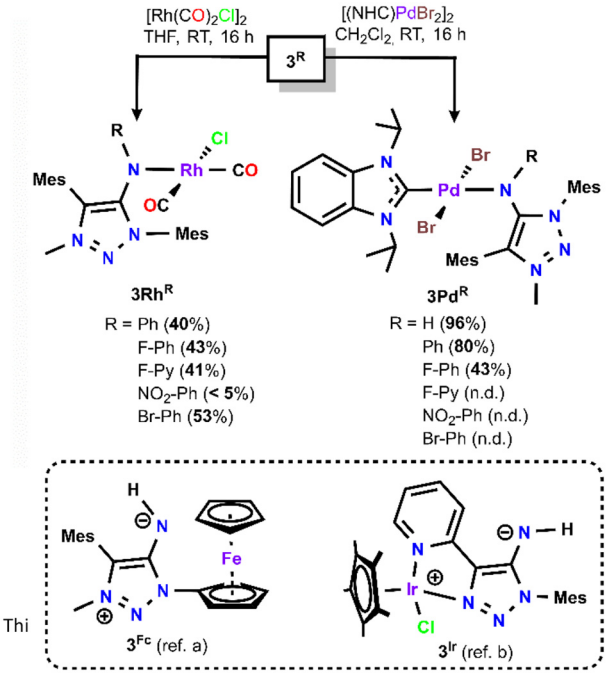

Scheme 4 Top: Synthesis of the Rh/Pd-complexes $\mathbf{3Rh^R}$/$\mathbf{3Pd^R}$ from the free MIIs $\mathbf{3^R}$. Bottom: Structure of previously reported MIIs. n.d. = not determined. References: a[26] and b.[27]

of all the other *hitherto* reported MIIs, highlighting the pronounced π-acidity of $\mathbf{3^{Ir}}$ compared to the other congeners.[17,27] As increased π-acidity will increase the TEP value and therefore imply a weaker net-electron donation, we assumed that the higher TEP value of $\mathbf{3^{Ir}}$ and $\mathbf{3^{Fc}}$ compared to $\mathbf{3^{H}}$ (which is a weaker nucleophile and base compared to $\mathbf{3^{Ir}}$/$\mathbf{3^{Fc}}$ according to reactivity studies and theoretical calculations) is the result of increased π-backbonding abilities of $\mathbf{3^{Ir}}$ and $\mathbf{3^{Fc}}$. The herein presented and discussed data therefore deliver further evidence that MIIs can act as π-acceptor ligands and that the flanking substituents heavily influence this accepting behaviour.

The HEPs were determined by examination of the corresponding chemical shifts of $C_{carbene}$ on the benzimidazole moiety by $^{13}C\{^1H\}$-NMR spectroscopy.[36] The HEP essentially follows the same trends as established by the theoretically calculated MCAs/HOMO–LUMO energy gaps and experimentally determined TEPs: the more electron-withdrawing the N_{exo} substituent, the lower the HEP and therefore the lower the σ-donation of the corresponding MII ligand. This trend is also apparent in the crystallographic data as the N4–Pd bond elongates in the sequence $\mathbf{3^{H}}$–$\mathbf{3^{Ph}}$–$\mathbf{3^{F\text{-}Ph}}$, while the Pd–$C_{Carbene}$ bond shortens in the same sequence.

The experimentally examined TEPs therefore highlight the strong donating propensity of MIIs as we already concluded in earlier works.[17,28] More so, the herein presented discussion offers a new indication that MIIs are also able to act as acceptor ligands. The HEPs determined for MIIs expanded the scale of donor strength in N donors, thus showing the strong donating properties of MIIs.[36]

Conclusions

In the presented work, we show how the N_{exo} substituent on MIIs influences the electronic structure and therefore the donor capabilities. To achieve this, we have presented two different ways to functionalise the N_{exo} position: the Buchwald–Hartwig amination was successfully employed on 5-amino-1,2,3-triazoles by the introduction of a Ph substituent

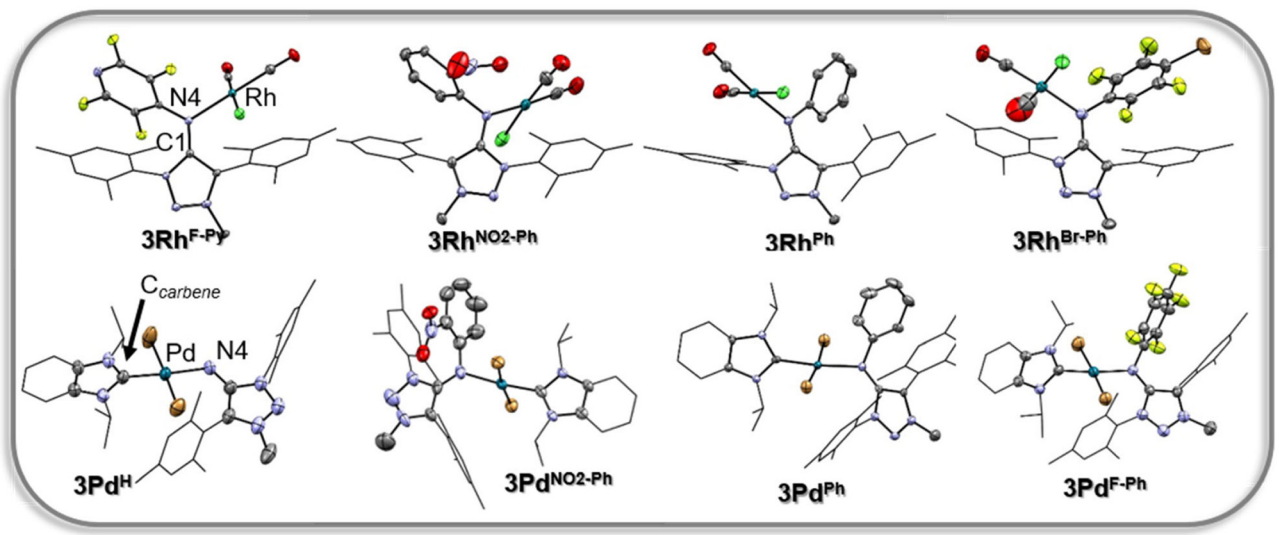

Fig. 5 Molecular structure in the crystal of the herein reported MII-Rh/Pd complexes obtained from sc-XRD (single-crystal X-ray diffraction) in the ORTEP representation. Thermal ellipsoids are set to 50% probability. Hydrogen atoms were omitted for clarity. Selected fragments are displayed in the wireframe representation for clarity.

Open Access Article. Published on 27 December 2024. Downloaded on 5/3/2026 5:07:20 PM. This article is licensed under a Creative Commons Attribution 3.0 Unported Licence.

on the amine. This approach highlights the versatility of 5-amino-1,2,3-triazoles as building blocks for MIIs. The triazole scaffold and also the N_{exo} position of MIIs can be adjusted by pre-functionalisation of the framework. The reaction of a free MII with electrophiles such as MeI and aromatic fluorides afforded the corresponding adducts. The reaction of the MII with MeI was not executed selectively and a product mixture was obtained. In contrast, we showed that MIIs are able to selectively activate aromatic C–F bonds at room temperature. Expanding this approach to different types of C–F bonds (and other electrophiles) opens up numerous possibilities for post-functionalisation of primary MIIs. The influence of the N_{exo} substituents on the electronic structure and donor properties was studied by a combination of crystallography, theoretical calculations and spectroscopy. From these studies, we can conclude that – unlike the flanking substituents on the triazole framework – the N_{exo} substituent has a strong effect on the donating ability of MIIs. Having established ways to functionalise the triazole core in previous works, we can now offer a more concise perspective on tuning the donor properties of MIIs. Such precise tuning of electronic properties should be useful for generating MIIs with tailor-made properties in the future.

Author contributions

RR and BS designed the project. All synthetic and spectroscopic studies were carried out by RR and AT. Single crystal X-ray diffraction data were solved and analysed by RR and HS. All DFT calculations were carried out by RR. The manuscript was written by RR and BS with inputs from the other authors.

Data availability

The data for this manuscript are available in the ESI.‡

Conflicts of interest

There are no conflicts to declare.

Acknowledgements

We want to thank Dr Falk Lissner, PD Ingo Hartenbach and Dr Wolfgang Frey for the measurement of X-ray diffraction data. Maren Barbara Neubrand is thanked for help with a crystallographic problem. We further want to thank Barbara Förtsch for elemental analyses and the analytical department of the Institute of Organic Chemistry of the University of Stuttgart for recording mass and NMR spectra. The present work made use of computational resources supported by the state of Baden-Württemberg through bwHPC and the German Research Foundation (DFG) through grant no. INST 40/575-1 FUGG (JUSTUS 2cluster). Apostolos Nektarios Agelidis is thanked for synthetic work during an internship.

References

1 R. Maity and B. Sarkar, *JACS Au*, 2022, **2**, 22–57.
2 Q. Liang and D. Song, *Dalton Trans.*, 2022, **51**, 9191–9198.
3 Á. Vivancos, C. Segarra and M. Albrecht, *Chem. Rev.*, 2018, **118**, 9493–9586.
4 D. Schweinfurth, L. Hettmanczyk, L. Suntrup and B. Sarkar, *Z. Anorg. Allg. Chem.*, 2017, **643**, 554–584.
5 J. J. Race and M. Albrecht, *ACS Catal.*, 2023, **13**, 9891–9904.
6 S. Chassaing, V. Bénéteau and P. Pale, *Catal. Sci. Technol.*, 2016, **6**, 923–957.
7 J. Hou, X. Liu, J. Shen, G. Zhao and P. G. Wang, *Expert Opin. Drug Discovery*, 2012, **7**, 489–501.
8 H. C. Kolb, M. G. Finn and K. B. Sharpless, *Angew. Chem., Int. Ed.*, 2001, **40**, 2004–2021.
9 H. C. Kolb and K. B. Sharpless, *Drug Discovery Today*, 2003, **8**, 1128–1137.
10 C. J. Hawker, V. V. Fokin, M. G. Finn and K. B. Sharpless, *Aust. J. Chem.*, 2007, **60**, 381.
11 J. M. Baskin, J. A. Prescher, S. T. Laughlin, N. J. Agard, P. V. Chang, I. A. Miller, A. Lo, J. A. Codelli and C. R. Bertozzi, *Proc. Natl. Acad. Sci. U. S. A.*, 2007, **104**, 16793–16797.
12 P. V. Chang, J. A. Prescher, E. M. Sletten, J. M. Baskin, I. A. Miller, N. J. Agard, A. Lo and C. R. Bertozzi, *Proc. Natl. Acad. Sci. U. S. A.*, 2010, **107**, 1821–1826.
13 M. Meldal and C. W. Tornøe, *Chem. Rev.*, 2008, **108**, 2952–3015.
14 G. Guisado-Barrios, M. Soleilhavoup and G. Bertrand, *Acc. Chem. Res.*, 2018, **51**, 3236–3244.
15 M. Albrecht, Chapter Two - Normal and Abnormal N-Heterocyclic Carbene Ligands: Similarities and Differences of Mesoionic C–Donor Complexes, in *Advances in Organometallic Chemistry*, ed. P. J. Pérez, Academic Press, 2014, pp. 111–158.
16 K. O. Marichev, S. A. Patil and A. Bugarin, *Tetrahedron*, 2018, **74**, 2523–2546.
17 R. Rudolf, N. I. Neuman, R. R. M. Walter, M. R. Ringenberg and B. Sarkar, *Angew. Chem., Int. Ed.*, 2022, **61**, e202200653.
18 D. Kase, T. Takada, N. Tsuji, T. Mitsuhashi and R. Haraguchi, *Asian J. Org. Chem.*, 2023, **12**, e202300108.
19 D. Kase and R. Haraguchi, *Org. Lett.*, 2022, **24**, 90–94.
20 S. Huang, Y. Wu, L. Huang, C. Hu and X. Yan, *Chem. – Asian J.*, 2022, **17**, e202200281.
21 A. Eitzinger, J. Reitz, P. W. Antoni, H. Mayr, A. R. Ofial and M. M. Hansmann, *Angew. Chem., Int. Ed.*, 2023, **62**, e202309790.
22 M. M. Hansmann, P. W. Antoni and H. Pesch, *Angew. Chem., Int. Ed.*, 2020, **59**, 5782–5787.
23 P. W. Antoni, J. Reitz and M. M. Hansmann, *J. Am. Chem. Soc.*, 2021, **143**, 12878–12885.

 This journal is © The Royal Society of Chemistry 2025

Open Access Article. Published on 27 December 2024. Downloaded on 5/3/2026 5:07:20 PM.
This article is licensed under a Creative Commons Attribution 3.0 Unported Licence.

24 Z. Zhang, S. Huang, L. Huang, X. Xu, H. Zhao and X. Yan, *J. Org. Chem.*, 2020, **85**, 12036–12043.
25 A. Das, P. Sarkar, S. Maji, S. K. Pati and S. K. Mandal, *Angew. Chem., Int. Ed.*, 2022, **61**, e202213614.
26 R. Rudolf and B. Sarkar, *Inorg. Chem.*, 2024, **63**, 23103–23117.
27 R. Rudolf and B. Sarkar, *ChemistryEurope*, 2025, **3**, e202400066.
28 R. Rudolf, D. Batman, N. Mehner, R. R. M. Walter and B. Sarkar, *Chem. – Eur. J.*, 2024, e202400730.
29 P. S. Gribanov, A. N. Philippova, M. A. Topchiy, L. I. Minaeva, A. F. Asachenko and S. N. Osipov, *Molecules*, 2022, **27**, 1999.
30 M. Pait, G. Kundu, S. Tothadi, S. Karak, S. Jain, K. Vanka and S. S. Sen, *Angew. Chem.*, 2019, **131**, 2830–2834.
31 B. Alič and G. Tavčar, *J. Fluor. Chem.*, 2016, **192**, 141–146.
32 S. Anga, S. Chandra, P. Sarkar, S. Das, D. Mandal, A. Kundu, H. Rawat, C. Schulzke, B. Sarkar, S. K. Pati, *et al.*, *EurJOC*, 2020, **2020**, 7445–7449.
33 D. Mandal, S. Chandra, N. I. Neuman, A. Mahata, A. Sarkar, A. Kundu, S. Anga, H. Rawat, C. Schulzke, K. R. Mote, *et al.*, *Chem. – Eur. J.*, 2020, **26**, 5951–5955.
34 N. Kuhn, R. Fawzi, M. Steimann, J. Wiethoff, D. Bläser and R. Boese, *Z. Naturforsch., B: Chem. Sci.*, 1995, **50**, 1779–1784.
35 H. V. Huynh, *Chem. Rev.*, 2018, **118**, 9457–9492.
36 Q. Teng and H. V. Huynh, *Dalton Trans.*, 2017, **46**, 614–627.